Yeast *PAH1*-encoded phosphatidate phosphatase controls the expression of *CHO1*-encoded phosphatidylserine synthase for membrane phospholipid synthesis

Received for publication, June 12, 2017, and in revised form, June 30, 2017 Published, Papers in Press, July 3, 2017, DOI 10.1074/jbc.M117.801720

Gil-Soo Han and George M. Carman[1]

From the Department of Food Science and the Rutgers Center for Lipid Research, New Jersey Institute for Food, Nutrition, and Health, Rutgers University, New Brunswick, New Jersey 08901

Edited by Dennis R. Voelker

The *PAH1*-encoded phosphatidate phosphatase (PAP), which catalyzes the committed step for the synthesis of triacylglycerol in *Saccharomyces cerevisiae*, exerts a negative regulatory effect on the level of phosphatidate used for the *de novo* synthesis of membrane phospholipids. This raises the question whether PAP thereby affects the expression and activity of enzymes involved in phospholipid synthesis. Here, we examined the PAP-mediated regulation of *CHO1*-encoded phosphatidylserine synthase (PSS), which catalyzes the committed step for the synthesis of major phospholipids via the CDP–diacylglycerol pathway. The lack of PAP in the *pah1*Δ mutant highly elevated PSS activity, exhibiting a growth-dependent up-regulation from the exponential to the stationary phase of growth. Immunoblot analysis showed that the elevation of PSS activity results from an increase in the level of the enzyme encoded by *CHO1*. Truncation analysis and site-directed mutagenesis of the *CHO1* promoter indicated that Cho1 expression in the *pah1*Δ mutant is induced through the inositol-sensitive upstream activation sequence (UAS_{INO}), a *cis*-acting element for the phosphatidate-controlled Henry (Ino2–Ino4/Opi1) regulatory circuit. The abrogation of Cho1 induction and PSS activity by a *CHO1* UAS_{INO} mutation suppressed *pah1*Δ effects on lipid synthesis, nuclear/endoplasmic reticulum membrane morphology, and lipid droplet formation, but not on growth at elevated temperature. Loss of the *DGK1*-encoded diacylglycerol kinase, which converts diacylglycerol to phosphatidate, partially suppressed the *pah1*Δ-mediated induction of Cho1 and PSS activity. Collectively, these data showed that PAP activity controls the expression of PSS for membrane phospholipid synthesis.

The *Saccharomyces cerevisiae*[2] *PAH1*-encoded PAP[3,4] (EC 3.1.3.4) and *CHO1*-encoded PSS[5] (EC 2.7.8.8) are two of the most highly regulated enzymes in lipid metabolism (1, 2). The PAP reaction is the committed step for the synthesis of the neutral lipid TAG, whereas the PSS reaction is the committed step in the CDP–DAG pathway for the *de novo* synthesis of the major membrane phospholipids PC and PE (1, 2) (Fig. 1). The DAG derived from the PAP reaction is also used in the CDP-choline and CDP-ethanolamine branches of the Kennedy pathway for the synthesis of PC and PE, respectively, when cells defective in PSS or other enzymes in the CDP–DAG pathway are supplemented with choline or ethanolamine (1, 2) (Fig. 1). For catalytic function, both Cho1 and Pah1 are required to associate with the membrane where their phospholipid substrates reside; Cho1 is an integral membrane enzyme in the ER (3–6), whereas Pah1 is a peripheral membrane enzyme that translocates from the cytosol to the nuclear/ER membrane (7–9).

Analyses of the *pah1*Δ and *cho1*Δ mutants lacking Pah1 and Cho1, respectively, have shed light on the importance of PAP and PSS activities in lipid metabolism and cell physiology. The *pah1*Δ mutation increases the level of the PAP substrate PA but decreases the levels of the PAP product DAG and its derivative TAG (10–12). The lack of Pah1 causes a variety of phenotypes that include the derepression of phospholipid synthesis genes (*e.g. INO1*, *OPI3*, and *INO2*), the increase of phospholipid synthesis, the expansion of the nuclear/ER membrane, the susceptibility to fatty acid-induced toxicity, and the reduction of lipid droplet formation (10–14). The impact of the Pah1 deficiency on overall cell physiology is further exemplified by the fact that *pah1*Δ mutant cells cannot grow on non-fermentable carbon sources (*i.e.* respiratory deficiency) (10, 15) as well as at elevated temperatures (10, 13, 15). The mutant cells are hypersensitive to oxidative stress, have a shortened chronological life span (16), and exhibit defects in cell wall integrity (17, 18) and vacu-

This work was supported, in whole or in part, by National Institutes of Health Grant GM028140. The authors declare that they have no conflicts of interest with the contents of this article. The content is solely the responsibility of the authors and does not necessarily represent the official views of the National Institutes of Health.

[1] To whom correspondence should be addressed: Dept. of Food Science, Rutgers University, 61 Dudley Rd., New Brunswick, NJ 08901. Tel.: 848-932-0267; E-mail: gcarman@rutgers.edu.

[2] In this paper, *Saccharomyces cerevisiae* is used interchangeably with yeast.

[3] The abbreviations used are: PAP, phosphatidate phosphatase; PSS, phosphatidylserine synthase; DGK, diacylglycerol kinase; DAG, diacylglycerol; TAG, triacylglycerol; PA, phosphatidate, PS, phosphatidylserine, PE, phosphatidylethanolamine; PC, phosphatidylcholine; PI, phosphatidylinositol; ER, endoplasmic reticulum; SC, synthetic complete; UAS, upstream activating sequence; UAS_{INO}, inositol-sensitive upstream activation sequence.

[4] The PAP encoded by *PAH1* differs from the lipid phosphate phosphatase enzymes encoded by *APP1* (83, 84), *DPP1* (85), and *LPP1* (86), which dephosphorylate a broad spectrum of substrates (*e.g.* PA, lyso-PA, DAG pyrophosphate, and isoprenoid pyrophosphate) and are not involved in *de novo* lipid synthesis.

[5] The *S. cerevisiae* PSS differs from the enzyme from Gram-negative bacteria (*e.g. E. coli*), which catalyzes its CDP–DAG–dependent reaction via a metal cofactor–independent ping-pong reaction mechanism (87), or the enzyme from mammalian cells, which catalyzes an exchange reaction between PC or PE and serine (88).

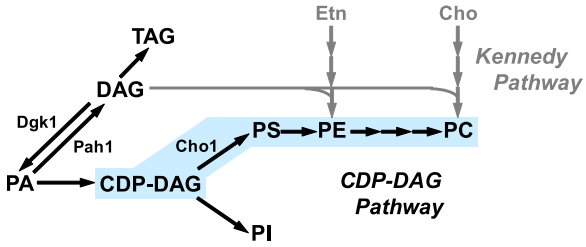

Figure 1. Lipid synthesis in yeast. The pathways shown for the synthesis of lipids include the relevant steps discussed in this work. A more comprehensive figure for the synthesis of TAG and membrane phospholipids via the CDP–DAG and Kennedy pathways may be found in Ref. 2. The CDP–DAG pathway of phospholipid synthesis is highlighted in *blue*, whereas the Kennedy pathway is shown in *gray* to indicate its minor role in phospholipid synthesis in cells grown without choline (*Cho*) or ethanolamine (*Etn*). The reactions catalyzed by the *CHO1*-encoded PSS, *PAH1*-encoded PAP, and *DGK1*-encoded DGK are indicated.

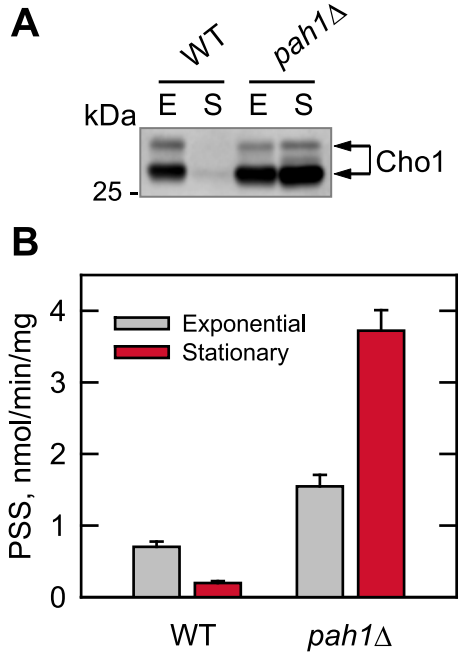

Figure 2. The *pah1*Δ mutation induces the expression of Cho1 and PSS activity. Wild type (W303-1A) and the *pah1*Δ mutant were grown at 30 °C in SC medium to the exponential (*E*) and stationary (*S*) phases. Cell extracts were prepared and assayed for the expression of Cho1 by immunoblot analysis with anti-Cho1 antibody (*A*) or for PSS activity (*B*). The immunoblot in *A* is representative of two independent experiments, whereas the data in *B* are means ± S.D. (*error bars*) from triplicate determinations of two independent experiments. The positions of the 30-kDa (*i.e.* phosphorylated) and 27-kDa (*i.e.* unphosphorylated) forms of Cho1 are indicated in *A*.

ole fusion (19). Some of the *pah1*Δ phenotypes require the function of Dgk1 (12, 14, 20), the CTP-dependent DGK that phosphorylates DAG to form PA (Fig. 1). The *cho1*Δ mutant lacks the ability to synthesize PS (21, 22) and thus requires the supplementation of choline or ethanolamine to synthesize PC or PE by the Kennedy pathway (1, 2). Studies with cells lacking Cho1 have revealed that PS is required for protein kinase C function (23, 24), tryptophan transport (25), vacuole function and morphogenesis (26), and direction of endocytic proteins to the plasma membrane (27).

Cho1 and Pah1 are regulated for their functions in lipid metabolism by genetic mechanisms. The expression of *CHO1* is elevated in the exponential phase when cells are grown in the absence of the phospholipid precursor molecules inositol, choline, ethanolamine, and serine (28–32) as well as in the presence of the essential nutrient zinc (33). In contrast, the *CHO1* expression is reduced by inositol supplementation in the exponential phase, and this regulation is enhanced by the addition of choline, ethanolamine, or serine in the growth medium (28–32). The gene expression is also reduced by zinc depletion from the growth medium (33) or when cells progress from the exponential to the stationary phase of growth (34, 35). These regulations of the *CHO1* expression are mediated by the Henry regulatory circuit, which involves the Ino2–Ino4 complex that drives transcriptional activation through its binding to the UAS_{INO} element and the PA-regulated repressor Opi1, which inhibits the function of the activator complex through its interaction with Ino2 (1, 2, 36). The *CHO1* transcriptional regulation plays a role in the partitioning of CDP–DAG for the synthesis of PI and PS and the PS-derived synthesis of PE and PC in the CDP–DAG pathway (1, 2, 36).

The expression of *PAH1* is also regulated by some of the same growth conditions that regulate the *CHO1* expression, but with an opposite effect (37–39). The transcriptional regulation of *PAH1* involves the transcription factors Ino2, Ino4, Opi1, Gis1, and Rph1 (for inositol and growth phase regulation) as well as the transcription factor Zap1 (for zinc-mediated regulation) (37–39). The induction of the *PAH1* transcription in the stationary phase or in response to zinc depletion correlates with the elevation of PAP activity (37, 38). On the one hand, the induced expression of PAP activity in zinc-replete stationary phase cells is responsible for increased synthesis and accumulation of TAG that occurs at the expense of phospholipid synthesis (37). On the other hand, the induced expression of PAP activity in zinc-depleted exponential phase cells is responsible for increased synthesis of PC via the CDP–choline branch of the Kennedy pathway (38).

The loss of Pah1 and its PAP activity (*e.g. pah1*Δ mutation) increases the level of PA and its utilization for the synthesis of membrane phospholipids (10, 37, 40), raising a question whether the expression of Cho1 and its PSS activity is regulated through cell growth. Here, we showed that the *pah1*Δ mutation results in the induction of Cho1 and PSS activity in a growth-dependent manner from the exponential to the stationary phase and that the elevation of the *CHO1* expression is controlled through the UAS_{INO} element in the promoter. The mutation in the core consensus of UAS_{INO} abolished the induction of Cho1 and PSS activity, resulting in the suppression of the *pah1*Δ phenotypes in lipid synthesis, nuclear/ER membrane morphology, and lipid droplet formation. Collectively, this work advances the understanding of how PAP activity regulates phospholipid synthesis through the transcriptional regulation of the PSS enzyme.

Results

*The pah1*Δ *mutation induces the expression of Cho1 and PSS activity*

We examined the effect of growth phase on the expression of *CHO1* and its encoded PSS activity in wild type and *pah1*Δ mutant cells (Fig. 2). In this work, the level of Cho1 was examined by immunoblotting to analyze the *CHO1* expression

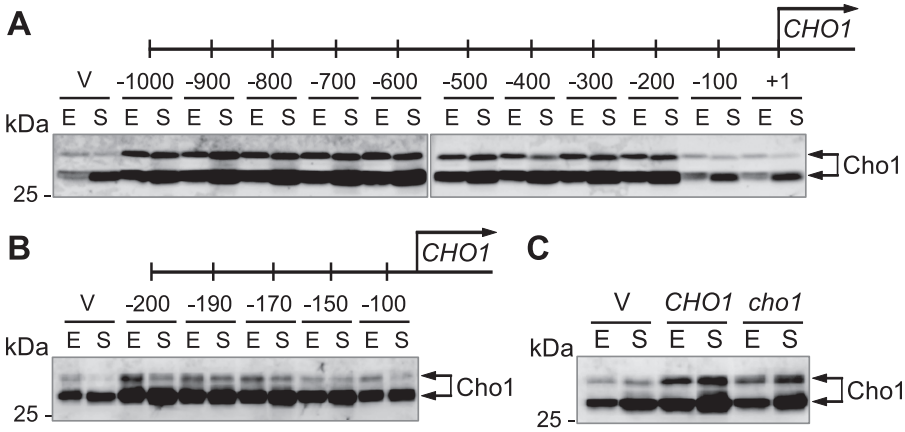

Figure 3. Induced expression of Cho1 in the *pah1*Δ mutant is mediated by the UAS_{INO} element in the *CHO1* promoter. *A* and *B*, the *pah1*Δ mutant was transformed with pRS415 (*V*), pGH440 (pRS415 + *CHO1* with 1,000-bp promoter), or its derivative with the indicated promoter truncation. *C*, the *pah1*Δ mutant was transformed with pRS415 (*V*), pGH440 (*CHO1*), or its derivative with the UAS_{INO} mutation (*cho1*). The transformants were grown at 30 °C in SC-Leu medium to the exponential (*E*) and stationary (*S*) phases. Cell extracts were prepared and subjected to immunoblot analysis with anti-Cho1 antibody. The immunoblots in the figure are representative of two independent experiments.

because of the caveat that mRNA abundance does not necessarily correlate with protein abundance. The anti-Cho1 antibody recognizes two forms of Cho1 that differ in their electrophoretic mobility (41). The 30-kDa form represents Cho1 phosphorylated by protein kinase A at Ser-46 and Ser-47, whereas the 27-kDa form represents the unphosphorylated form of the enzyme (41). In wild-type cells, the levels of Cho1 (Fig. 2*A*) and its PSS activity (Fig. 2*B*) were reduced in the stationary phase when compared with the exponential phase. As described previously (34), PSS activity was 3.6-fold lower in the stationary phase than in the exponential phase. Compared with wild type, the *pah1*Δ mutant had 2.2-fold higher PSS activity in the exponential phase. In addition, the *pah1*Δ mutant showed a 2.4-fold induction of the enzyme activity from the exponential to the stationary phase. Consequently, in the stationary phase, the PSS activity of the *pah1*Δ mutant was 19-fold higher than the enzyme activity of wild type. The elevation of PSS activity in the *pah1*Δ mutant correlated with the increase of the Cho1 level. These results indicate that the induced expression of Cho1 and PSS activity in the *pah1*Δ mutant is up-regulated during growth from the exponential to the stationary phase.

*Induced expression of Cho1 and PSS activity in the pah1*Δ *mutant is mediated by the CHO1 UAS_{INO} element*

The up-regulation of the Cho1 level in the *pah1*Δ mutant suggested that the enzyme is controlled at the level of its gene expression. The *CHO1* promoter contains a UAS_{INO} element as well as other putative regulatory elements. To identify the relevant element by an unbiased approach, we constructed *CHO1* alleles that contain different lengths of the promoter by 5′-nested deletion and analyzed their expression on a low-copy plasmid in the *pah1*Δ mutant. We reasoned that if the plasmid-borne *CHO1* allele contains a UAS, its expression would be up-regulated like the endogenous expression of Cho1 in the *pah1*Δ mutant. We did not analyze the plasmid-borne *CHO1* alleles in the *cho1*Δ *pah1*Δ mutant background. Supplementation of choline or ethanolamine, which is required for viability of cells containing the *cho1*Δ mutation, alters the regulation of phospholipid synthesis (21, 22). Accordingly, *pah1*Δ cells transformed with the *CHO1* allele were grown to the exponential and stationary phases and were examined for the Cho1 level by immunoblot analysis (Fig. 3). Compared with the *pah1*Δ mutant that expresses the endogenous *CHO1* (*i.e.* vector control), its transformants containing the *CHO1* allele with the 200-bp or longer promoter exhibited higher levels of Cho1 in both the exponential and the stationary phases of growth (Fig. 3*A*). However, the increase of the Cho1 level was not shown by the expression of the *CHO1* allele with the 100-bp or shorter promoter, indicating that the UAS element is located between −200 and −100 of the *CHO1* promoter. Further truncation analysis of the 100-bp region showed that the Cho1 level of the *pah1*Δ mutant was increased by the *CHO1* allele with the 170-bp or longer promoter, but not with the 150-bp promoter (Fig. 3*B*), indicating that the UAS element affecting expression is located between −170 and −150. Analysis of the 20-bp region of the *CHO1* promoter revealed that it contains the UAS_{INO} element (−163 to −154).

To determine whether the UAS_{INO} element is required for the induction of *CHO1* expression in the *pah1*Δ mutant, we examined the effect of its mutation (CATGTGAAAG → TTTTTTAAAG, mutations underlined) (42) in the plasmid-borne *CHO1*. Compared with the wild type allele, the mutant allele of *CHO1* lacking the consensus sequence of UAS_{INO} did not significantly increase the Cho1 level in the *pah1*Δ mutant (Fig. 3*C*). To further confirm this result, the UAS_{INO} mutation was introduced to the chromosomal *CHO1* of wild type and the *pah1*Δ mutant. Immunoblot analysis (Fig. 4*A*) showed that the *cho1* mutant had a significant reduction of the Cho1 level in the exponential phase. Compared with the *pah1*Δ mutant, the *cho1 pah1*Δ mutant showed a great reduction of the Cho1 level in the exponential and stationary phases (Fig. 4*A*). In fact, its Cho1 level was almost identical to that of the *cho1* mutant. The effect of the UAS_{INO} mutation on the Cho1 level correlated with the decrease of PSS activity (Fig. 4*B*). In the exponential phase, PSS activity of the *cho1 pah1*Δ mutant was 5.2- and 8.4-fold, respectively, lower than that of wild type and the *pah1*Δ mutant; in the stationary phase, the enzyme activity was

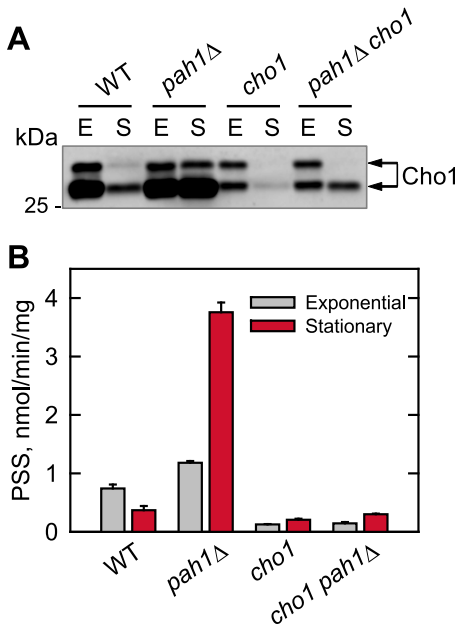

Figure 4. The inductions of Cho1 and PSS activity in the *pah1*Δ mutant are abolished by the *CHO1* UAS_{INO} mutation. Wild type, the *pah1*Δ mutant, and their derivatives containing the chromosomal *CHO1* UAS_{INO} mutation (*cho1*) were grown at 30 °C in SC medium to the exponential (*E*) and stationary (*S*) phases. Cell extracts were prepared and assayed for the expression of Cho1 by immunoblot analysis with anti-Cho1 antibody (*A*) or for PSS activity (*B*). The immunoblot in *A* is representative of two independent experiments, whereas the data in *B* are means ± S.D. (*error bars*) from triplicate determinations of two independent experiments. The positions of the 30-kDa (*i.e.* phosphorylated) and 27-kDa (*i.e.* unphosphorylated) forms of Cho1 are indicated in *A*.

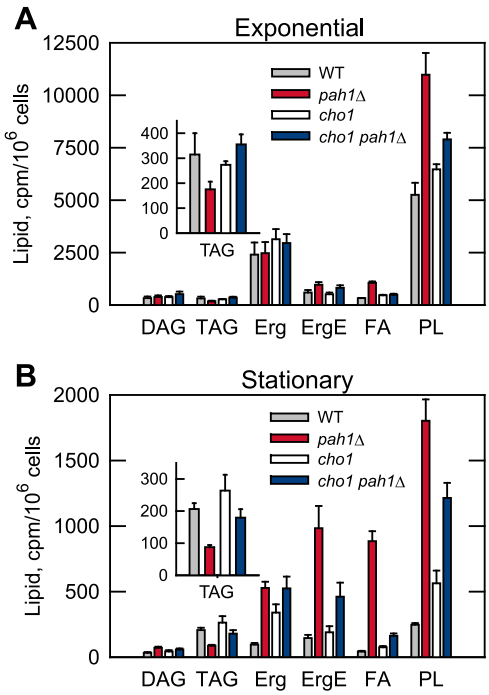

Figure 5. Effect of the *CHO1* UAS_{INO} mutation on lipid composition in the *pah1*Δ mutant. Wild type, the *pah1*Δ mutant, and their derivatives containing the chromosomal *CHO1* UAS_{INO} mutation (*cho1*) were grown at 30 °C in SC medium to the exponential (*A*) and stationary (*B*) phases of growth in the presence of [2-^{14}C]acetate (1 μCi/ml). Lipids were extracted and separated by the one-dimensional thin-layer chromatography system for neutral lipids, and the images were subjected to ImageQuant analysis. The data are reported as counts/min found in a particular lipid per 10^6 cells. The amount of label found in the lipids from the stationary phase cultures was reduced relative to that found from the exponential phase because of the turnover of lipids during growth and incorporation of the label into other metabolites. The data are means ± S.D. (*error bars*) from triplicate determinations. *Erg*, ergosterol; *ErgE*, ergosterol ester; *FA*, fatty acid; *PL*, phospholipids.

1.2- and 12-fold, respectively, lower than that of wild type and the *pah1*Δ mutant. Taken together, these results indicate that the UAS_{INO} element is responsible for the induction of Cho1 expression in the *pah1*Δ mutant and its growth-dependent up-regulation from the exponential to the stationary phase.

*Effects of the CHO1 UAS_{INO} mutation on lipid composition of the pah1*Δ *mutant*

We explored the effects of the *CHO1* UAS_{INO} mutation on the changes of lipid composition imparted by the *pah1*Δ mutation. Yeast cells were grown in SC medium containing [2-^{14}C]acetate for steady-state labeling of lipids (43, 44). The radiolabeled lipids were extracted from exponential and stationary phase cells and analyzed by TLC for total lipids and phospholipids. As described previously (12), the *pah1*Δ mutant had a reduced level of TAG (1.8- and 2.4-fold, respectively) but an increased level of phospholipids (2.1- and 7.8-fold, respectively) in the exponential and stationary phases (Fig. 5). The alterations in the levels of TAG and phospholipids were suppressed by the *CHO1* UAS_{INO} mutation in the exponential phase (Fig. 5*A*) and partially suppressed in the stationary phase (Fig. 5*B*). In addition, the *pah1*Δ mutation caused a high increase in the levels of sterol esters (6.7-fold) and fatty acids (20-fold) in the stationary phase (10, 37). These effects of the *pah1*Δ mutation were also suppressed by the *CHO1* UAS_{INO} mutation (Fig. 5*B*). As for individual phospholipid species, the *pah1*Δ mutant showed an increase in the levels of PC (1.9- and 13.4-fold), PE (3- and 6-fold), PI (2.5- and 7.8-fold), PS (1.5- and 6.4-fold), and PA (2.4- and 6-fold) in the exponential (Fig. 6*A*) and stationary (Fig. 6*B*) phases, respectively. The *CHO1* UAS_{INO} mutation suppressed the *pah1*Δ-mediated increase in the levels of PC, PE, PS, and PA in the exponential phase but had little effect on the level of PI.

*Effects of the CHO1 UAS_{INO} mutation on nuclear/ER membrane morphology, lipid droplet formation, and temperature sensitivity of the pah1*Δ *mutant*

The *pah1*Δ mutant has an irregularly shaped nucleus with the expansion of the membrane that is attributed to the increase of phospholipid synthesis (11, 13). Because the *CHO1* UAS_{INO} mutation exerts a suppressive effect on the *pah1*Δ-mediated increase of phospholipid synthesis, we examined the nuclear/ER membrane morphology of the *cho1 pah1*Δ mutant (Fig. 7*A*). The expression of the Sec63-GFP fusion protein was used to mark the nuclear/ER membrane in the cell (13). Compared with wild type, the *cho1* mutant showed little difference in the nuclear/ER membrane morphology and contained a round nucleus. As described previously (13), most of the *pah1*Δ cells showed the irregular, expanded nuclear/ER morphology. In contrast, the *cho1 pah1*Δ cells (93%; Fig. 7*B*) had the round-shaped nucleus in the exponential phase, indicating that the *CHO1* UAS_{INO} mutation suppresses the nuclear/ER membrane phenotype of the *pah1*Δ mutant. The suppressive effect was less strong in the stationary phase, and the number of *cho1 pah1*Δ cells containing a round nucleus was reduced by 53%.

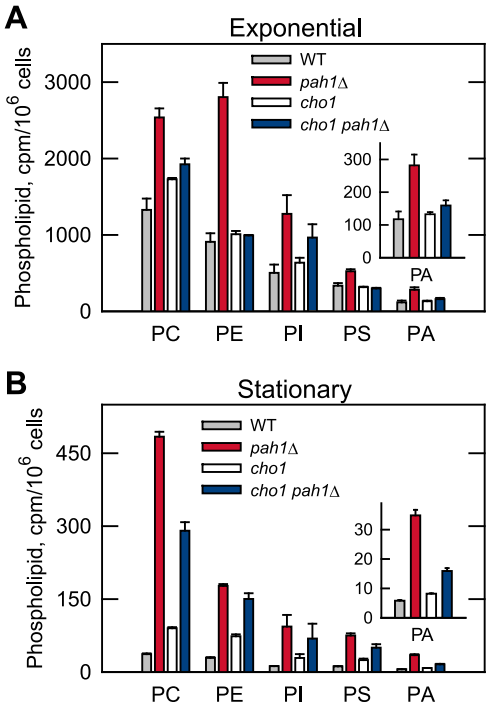

Figure 6. Effect of the *CHO1* UAS_{INO} mutation on phospholipid composition in the *pah1*Δ mutant. Wild type, the *pah1*Δ mutant, and their derivatives containing the chromosomal *CHO1* UAS_{INO} mutation (*cho1*) were grown at 30 °C in SC medium to the exponential (*A*) and stationary (*B*) phases of growth in the presence of [2-^{14}C]acetate (1 μCi/ml). Lipids were extracted and separated by the one-dimensional thin-layer chromatography system for phospholipids, and the images were subjected to ImageQuant analysis. The data are reported as counts/min found in a particular lipid per 10^6 cells. The amount of label found in the phospholipids from the stationary phase cultures was reduced relative to that found from the exponential phase because of the turnover of lipids during growth and incorporation of the label into other metabolites. The data are means ± S.D. (*error bars*) from triplicate determinations.

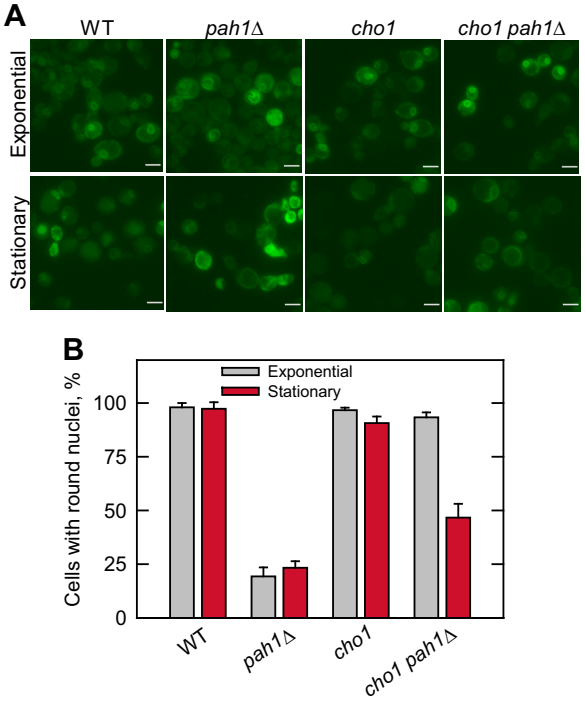

Figure 7. Effect of the *CHO1* UAS_{INO} mutation on nuclear/ER membrane morphology in the *pah1*Δ mutant. Wild type, the *pah1*Δ mutant, and their derivatives containing the chromosomal *CHO1* UAS_{INO} mutation (*cho1*) were transformed with YCplac111-*SEC63-GFP* and grown at 30 °C in SC-Leu medium to the exponential and stationary phases. *A*, the fluorescence signal of the GFP-tagged ER marker Sec63 was visualized by fluorescence microscopy. The images shown are representative of multiple fields of view. *White bar*, 2 μm. *B*, the percentage of cells with round nuclear/ER membrane morphology was determined from ≥3 fields of view (≥150 cells). The data are averages ± S.D. (*error bars*).

We also examined the mutants for the formation of lipid droplets by staining with the fluorescent dye BODIPY 493/503 (Fig. 8*A*). The wild-type and *cho1* cells had a similar number of lipid droplets and showed a ~1.5-fold increase in the organelle number from the exponential to the stationary phase (Fig. 8*B*). Compared with wild type, the *pah1*Δ mutant showed a significant reduction (2- and 4.5-fold, respectively) of lipid droplet formation in the exponential and stationary phases. In addition, its lipid droplet formation was not increased in the stationary phase. This phenotype of the *pah1*Δ mutant was suppressed by the *CHO1* UAS_{INO} mutation, and the *cho1 pah1*Δ mutant had a number of lipid droplets similar to that of the wild type in the exponential phase. In the stationary phase, the *cho1 pah1*Δ mutant showed a reduction in lipid droplet formation, but its lipid droplet number was still higher than that of wild type. This result indicates that, in the stationary phase of growth, the *CHO1* UAS_{INO} mutation has a partial suppressive effect on the defect of the *pah1*Δ mutant in lipid droplet formation.

The lack of growth at the elevated temperature (*e.g.* 37 °C) is characteristic of the *pah1*Δ mutant (10, 13, 15). Unlike the phenotypes described above, temperature sensitivity of the *pah1*Δ mutant in the exponential and stationary phases was not suppressed by the *CHO1* UAS_{INO} mutation (Fig. 9).

*Effect of the dgk1*Δ *mutation on the induced expression of Cho1 and PSS activity of the pah1*Δ *mutant*

The lack of Dgk1 (*i.e.* the *dgk1*Δ mutation) suppresses the *pah1*Δ phenotypes (*e.g.* increased phospholipid synthesis, nuclear/ER membrane expansion, and induced *INO1* expression) that correlate with an increase in the PA level (20, 20). Accordingly, we examined the effect of the *dgk1*Δ mutation on the Cho1 expression and PSS activity of wild type and the *pah1*Δ mutant (Fig. 10). The *dgk1*Δ mutation introduced into wild type did not have a major effect on the expression of Cho1 (Fig. 10*A*) and PSS activity (Fig. 10*B*). In contrast, it showed a partial suppressive effect on the Cho1 expression and PSS activity of the *pah1*Δ mutant in the stationary phase, but not in the exponential phase. For example, the PSS activity of the *dgk1*Δ *pah1*Δ mutant in the stationary phase was 32% lower than that of the *pah1*Δ mutant. Yet, the PSS activity of the double mutant was 7-fold higher than the enzyme activity of wild type in the stationary phase.

Because both PAP and DGK control the PA level (10, 20), we examined the effect of the *dgk1*Δ mutation on the PA level of the *pah1*Δ mutant. As described previously (12, 20), the *pah1*Δ mutation caused an increase in the PA content in both the exponential (2.2-fold) and stationary (2.7-fold) phases of growth. The *dgk1*Δ mutation suppressed the *pah1*Δ effect on PA content (Fig. 10*C*). We also examined the effect of the *dgk1*Δ mutation on temperature sensitivity exhibited by the *pah1*Δ

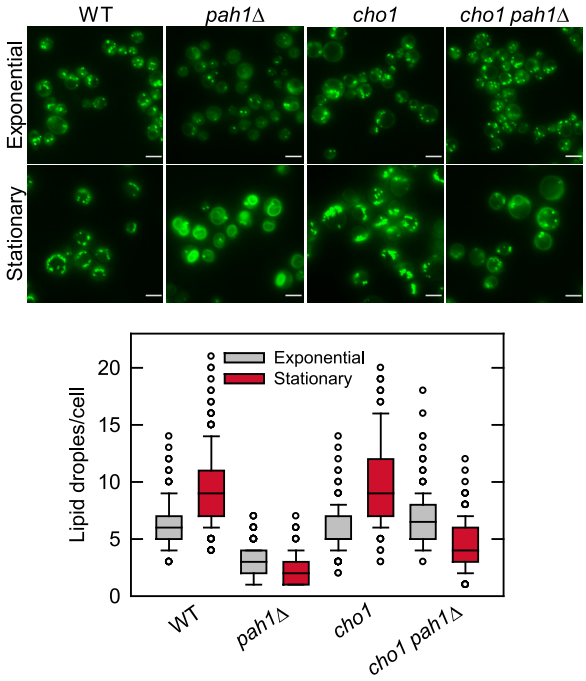

Figure 8. Effect of the *CHO1* UAS_{INO} mutation on lipid droplet formation in the *pah1*Δ mutant. Wild type, the *pah1*Δ mutant, and their derivatives containing the chromosomal *CHO1* UAS_{INO} mutation (*cho1*) were grown at 30 °C in SC medium to the exponential and stationary phases followed by staining with BODIPY 493/503. *A*, the stained lipid droplets were visualized by fluorescence microscopy. The images shown are representative of multiple fields of view. *White bar*, 2 μm. *B*, the number of lipid droplets was counted from ≥3 fields of view (≥150 cells) and presented by a box plot with the 5th and 95th percentile.

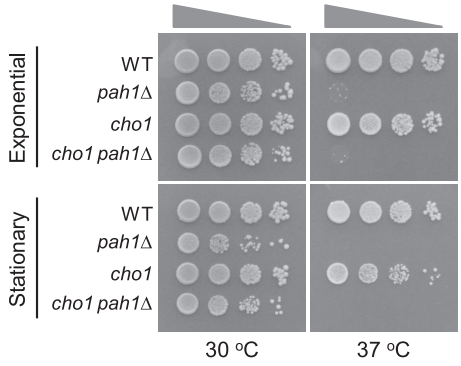

Figure 9. Effect of the *CHO1* UAS_{INO} mutation on growth at 37 °C in the *pah1*Δ mutant. Wild type, the *pah1*Δ mutant, and their derivatives containing the chromosomal *CHO1* UAS_{INO} mutation (*cho1*) were grown at 30 °C in YEPD medium to saturation. Serial dilutions (1:10) of the cells were spotted (5 μl) onto YEPD plates, and growth was scored after 3 days of incubation at 30 and 37 °C. The data are representative of three independent experiments.

mutant. Like the *pah1*Δ mutant, the *dgk1*Δ *pah1*Δ mutant showed no growth at 37 °C, indicating that temperature sensitivity of the *pah1*Δ mutant is not suppressed by the loss of DGK activity (Fig. 10*D*).

Discussion

PAP and PSS catalyze reactions in the overlapping pathways of lipid biosynthesis (Fig. 1). The enzyme reactions are linked to the lipid intermediate PA, which is the substrate of PAP and the precursor of CDP–DAG used as the substrate of PSS (Fig. 1). The conversion of PA to DAG and CDP–DAG appears to be a major regulatory step that bifurcates the lipid biosynthetic pathway into two branches (*i.e.* TAG synthesis and phospholipid synthesis) (10, 12, 37). The changes in PAP activity are directly correlated with TAG synthesis but are inversely correlated with phospholipid synthesis during cell growth (37). Accordingly, yeast cells have a lower PAP activity in the exponential phase when the rate of phospholipid synthesis is high, whereas they have a higher PAP activity in the stationary phase when the rate of phospholipid synthesis is low (37). The elevation of phospholipid synthesis in the *pah1*Δ mutant, which causes the expansion of the nuclear/ER membrane, is related to the increased availability of the precursor PA by the defect of its conversion to DAG as well as by the increased expression of phospholipid synthesis genes (10, 12, 13). We showed in this study that the expression of *CHO1*-encoded PSS, which catalyzes the committed step in the CDP–DAG pathway of *de novo* phospholipid synthesis, is highly induced in the *pah1*Δ mutant and that the enzyme induction is increased in the stationary phase when the *CHO1* expression in wild type is reduced. That the induction of *CHO1* expression in the *pah1*Δ mutant was mediated through the UAS_{INO} element supports the notion that the elevation of the PA level reduces the Opi1-mediated transcriptional repression of the UAS_{INO}-containing genes as per the Henry regulatory circuit (Fig. 11). PA is known to sequester Opi1 at the nuclear/ER membrane (2, 45), and the phospholipid synthesis genes (*e.g. INO1*, *INO2*, and *OPI3*) previously known to be induced by the *pah1*Δ mutation (13) contain the UAS_{INO} element (2, 46, 47).

The *CHO1* UAS_{INO} mutation in the *pah1*Δ mutant abolished the up-regulation of the Cho1 level and PSS activity, suppressing the increase of phospholipid synthesis and nuclear/ER membrane as well as the decrease of TAG synthesis and lipid droplet formation. These observations highlight the role of the *CHO1*-encoded PSS in the synthesis of membrane phospholipids and the role of the *PAH1*-encoded PAP in the negative regulation of the *CHO1* expression. The effects of the *CHO1* UAS_{INO} mutation on the *pah1*Δ phenotypes were pronounced in the exponential phase of growth when PSS activity is expressed at its highest level (34). The partial suppression of the *pah1*Δ phenotypes in the stationary phase suggests that the higher availability of PA may compensate for the reduction of the PSS level.

Although the PA level of the *pah1*Δ mutant was reduced by the *CHO1* UAS_{INO} mutation in the stationary phase, it was still higher than that of wild type cells (Fig. 6*B*). This difference in the PA content would be expected to attenuate the Opi1 function. As indicated above, it has been known that transcription of other UAS_{INO}-containing phospholipid synthesis genes (*e.g. INO1* and *OPI3*) is induced in the *pah1*Δ mutant (13, 48). Although it is unknown whether transcriptional induction of these genes leads to the increased expression and function of their encoded proteins, the lack of total suppression of PC content, especially in the stationary phase, is consistent with an increase in phospholipid methyltransferase activity encoded by *OPI3*. Phospholipid synthesis genes (*e.g. CKI1* (49), *CPT1* (50), *EKI1* (51), and *EPT1* (52)) in the Kennedy pathway are also subject to transcriptional regulation through the UAS_{INO} element, but their encoded activities are not expected to play a

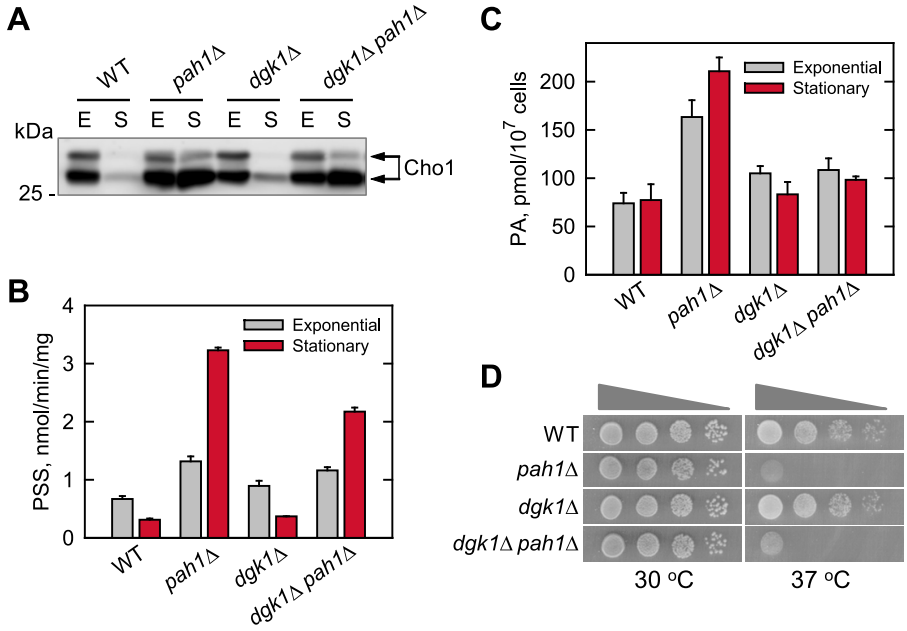

Figure 10. Effect of the *dgk1*Δ mutation on the *pah1*Δ mutant for its induced expressions of Cho1 and PSS activity, PA content, and temperature sensitivity. Wild type (RS453) and the indicated mutants were grown at 30 °C in SC medium to the exponential (*E*) and stationary (*S*) phases. Cell extracts were prepared and assayed for the expression of Cho1 by immunoblot analysis with anti-Cho1 antibody (*A*) or for PSS activity (*B*). Lipids extracted from the cells in the exponential and stationary phases were digested with lipoprotein lipase, and glycerol 3-phosphate produced from PA was measured by the fluorometric coupled enzyme assay (*C*). *D*, wild type and the indicated mutants were grown at 30 °C in YEPD medium to saturation. Serial dilutions (1:10) of the cells were spotted (5 μl) onto YEPD plates, and growth was scored after 3 days of incubation at 30 and 37 °C. The immunoblot in *A* and the cell growth in *D* are representative of two independent experiments, whereas the data in *B* and *C* are means ± S.D. (*error bars*) from triplicate determinations of two independent experiments. The positions of the 30-kDa (*i.e.* phosphorylated) and 27-kDa (*i.e.* unphosphorylated) forms of Cho1 are indicated in *A*.

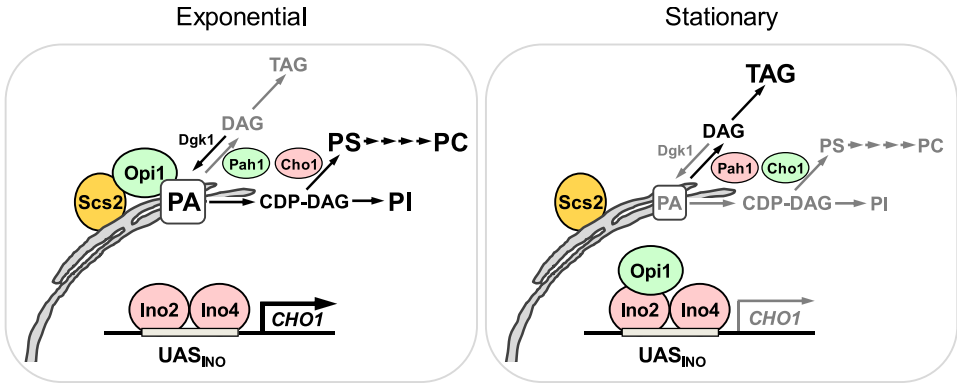

Figure 11. Model for the Pah1-mediated regulation of Cho1 expression and lipid synthesis during growth. The diagram shows the Henry regulatory circuit, which includes the repressor Opi1, the Ino2–Ino4 activator complex, and the UAS_{INO} element in *CHO1* (2), and the bifurcation of PA for the synthesis of TAG and phospholipids via the CDP–DAG pathway. Under growth conditions (*e.g.* exponential phase; *left*) whereby Pah1 expression (*green highlight*) and PAP activity are low (37), the level of PA is elevated, and the Opi1 repressor is tethered to the nuclear/ER membrane via its interactions with PA and Scs2. The inhibition of Opi1 for its nuclear entry allows for the transcriptional activation (*boldface arrow*) of *CHO1* by the Ino2–Ino4 complex and the inductions of Cho1 (*pink highlight*) and PSS activity for increased phospholipid synthesis (*large letters*) via the CDP–DAG pathway (this work). The reduced rate of TAG synthesis in the exponential phase of growth (37) is indicated with *small gray letters*. Under growth conditions (*e.g.* stationary phase; *right*) whereby Pah1 expression (*pink highlight*) and PAP activity are high (37), the synthesis of TAG is elevated (*large letters*) and the PA level is reduced (*small gray letters*). The reduction of the PA level allows for the dissociation of Opi1 from the nuclear/ER membrane and its entry into the nucleus, where it represses the transcriptional activation of *CHO1* (*thin gray arrow* and *letters*) by inhibiting the function of the Ino2–Ino4 activator complex through its binding to Ino2. The repression of Cho1 (*green highlight*) and PSS activity results in the reduction of phospholipid synthesis (*small gray letters*).

major role in this regulation because growth medium was not supplemented with choline and/or ethanolamine (1, 2).

The increase of the PI content in the *pah1*Δ mutant was not suppressed by the *CHO1* UAS_{INO} mutation in the exponential or stationary phase of growth. Whereas the expression of *PIS1*-encoded PI synthase is not regulated through Opi1 (28, 53), the *INO1* gene encoding the inositol-3-phosphate synthase, which is crucial for the synthesis of inositol and thus for PI synthesis (54), is regulated by Opi1 (28, 55). Thus, the induced expression of *INO1* in response to the *pah1*Δ mutation (13) is consistent with the increased availability of inositol for PI synthesis. However, if the induced expression of *INO1* is translated to an increase in the level and activity of inositol-3-phosphate synthase, it would not be massive because *pah1*Δ mutant cells do not excrete inositol (10).

The *pah1*Δ mutation also causes a dramatic increase in the amounts of fatty acids and ergosterol ester, primarily in the stationary phase of growth (10) (Fig. 5). Although the mecha-

nism for these changes is unclear, the elevated levels of the lipids were almost reduced to the levels of wild type by alleviating the induced expression of PSS activity. We hypothesize that the PA content, as regulated by the *pah1*Δ and *cho1 pah1*Δ mutations, is the basis for the changes in the levels of fatty acids and ergosterol ester. This assertion is supported by the fact that fatty acid synthesis, as mediated by the *ACC1*, *FAS1*, and *FAS2* genes, is under the control of the Henry regulatory circuit (56, 57) and that the *ARE1* and *ARE2* genes, which encode the acyl-CoA sterol acyltransferase enzymes, contain a putative UAS_{INO} element in their promoters. Accordingly, additional studies are warranted to addresses the expression regulation of those genes.

The lack of the *DGK1*-encoded DGK suppresses the *pah1*Δ phenotypes that are ascribed to the increase of the PA level (20, 58), which include the induced expression of UAS_{INO}-containing genes and increased phospholipid content, nuclear/ER membrane expansion, decreased lipid droplet formation, and reduced chronological life span (10, 12–14, 16, 20, 59). As discussed above, we consider that the increase of the PA level is responsible for induced expression of Cho1 and PSS activity in the *pah1*Δ mutant. In further support of this, we showed that the *dgk1*Δ mutation suppressed the *pah1*Δ mutant for its induced Cho1 expression and PSS activity, but only in the stationary phase of growth with a partial effect. Thus, the PA-mediated regulation of the *CHO1* expression is more complex than was expected.

Of the *pah1*Δ phenotypes examined in this study, temperature sensitivity was not suppressed by the *CHO1* UAS_{INO} mutation or by the *dgk1*Δ mutation. These observations support the notion that the inability of the *pah1*Δ mutant to grow at the elevated temperature is not related to a change in the PA level but rather to other changes (*e.g.* decrease in DAG production) caused by the loss of PAP activity. Additional *pah1*Δ phenotypes that are not affected by the *dgk1*Δ mutation include the decrease of TAG synthesis, sensitivity to fatty acid toxicity (12), and vacuole fragmentation (60).

In addition to the genetic regulation discussed above, the PAP and PSS activities of Pah1 and Cho1, respectively, are biochemically regulated by the substrates and products of their reactions. The PSS substrate CDP–DAG stimulates PAP activity by a mechanism that increases its affinity for PA (61), whereas the PAP substrate PA stimulates PSS activity by a mechanism that increases its affinity for CDP–DAG (62). Moreover, the PAP product DAG inhibits PSS activity by a noncompetitive mechanism (62). The two enzymes are also regulated by phosphorylation. Protein kinase A phosphorylates Pah1 (63) and Cho1 (41, 64) and inhibits their PAP and PSS, activities, respectively. For Cho1, the posttranslational modification stabilizes its abundance in the cell for the net effect of stimulating the synthesis of PS (41). The phosphorylation-mediated regulations of the two enzymes are more complex and are discussed elsewhere (1). In addition, the regulations of Pah1 and Cho1 are interrelated with the metabolism of nucleotides and sphingolipids (1, 2, 65).

In summary, the work reported here advances our understanding of how the PAP enzyme reaction regulates phospholipid synthesis through the transcriptional regulation of the PSS enzyme. Clearly, the long-term genetic regulations, coupled with the short-term biochemical regulations of the PAP and PSS enzymes are critical to controlling the balance between the synthesis of TAG for stasis and the synthesis of membrane phospholipids for cell growth.

Experimental procedures

Materials

All chemicals were reagent grade or better. Culture medium components were from BD Difco. DNA purification kits were from Qiagen. Restriction endonucleases, modifying enzymes, and DNA polymerases were from New England Biolabs. DNA size standards (1 Kb Plus DNA ladder) were from Invitrogen. Oligonucleotides, nucleotides, protease inhibitors, Triton X-100, Ponceau S stain, *Aerococcus viridans* glycerol-3-phosphate oxidase, horseradish peroxidase, and bovine serum albumin were from Sigma-Aldrich. Carrier DNA for yeast transformation was from Clontech. Bradford protein assay reagent, protein size standards, and electrophoretic reagents were from Bio-Rad. PVDF membrane and the enhanced chemifluorescence substrate for Western blotting were from GE Healthcare. Alkaline phosphatase–conjugated goat anti-rabbit IgG antibodies (product 31340, lot NJ178812), alkaline phosphatase-conjugated goat anti-mouse IgG antibodies (product 31322, lot PB1815636), Triton X-100 (Surfact-Amps, product 28314), Amplex Red, and BODIPY 493/503 were from Thermo Fisher Scientific. *Pseudomonas* sp. lipoprotein lipase was from Wako. Radiochemicals were from PerkinElmer Life Sciences. Phospholipids were from Avanti Polar Lipids. Liquid scintillation mixtures were from National Diagnostics. Silica gel 60 TLC plates were from EMD Millipore, and LK5D partisil silica gel TLC plates were from Whatman.

Strains and growth conditions

The strains used in this work are listed in Table 1. Yeast cells were grown at 30 °C in YEPD medium (1% yeast extract, 2% peptone, 2% glucose) or in SC medium containing 2% glucose (66). For selection of yeast cells containing plasmids, appropriate amino acids were omitted from SC medium. *Escherichia coli* DH5α was used for plasmid maintenance and amplification and was grown at 37 °C in LB medium (1% tryptone, 0.5% yeast extract, 1% NaCl, pH 7.4). *E. coli* transformants containing plasmids were selected by ampicillin (100 μg/ml) resistance. Solid media for the growth of *E. coli* and yeast contained agar at a concentration of 1.5 and 2%, respectively. Cell numbers in liquid cultures were estimated spectrophotometrically by measuring absorbance at 600 nm.

DNA manipulations

Standard methods were used for the isolation of plasmid and yeast genomic DNA and for the manipulation of DNA with restriction enzymes, DNA ligase, and modifying enzymes (66, 67). PCRs were optimized as described by Innis and Gelfand (68). Yeast and *E. coli* transformations were performed by standard protocols. DNA sequencing reactions were performed according to the dideoxy method with *Taq* DNA polymerase and analyzed by automated DNA sequencer (service provided by GENEWIZ, South Plainfield, NJ).

Table 1
Strains used in this study

Strain	Relevant characteristics	Source/Reference
E. coli		
DH5α	F$^-$ ϕ80d*lacZ*ΔM15Δ (*lacZYA-argF*)U169 *deoR recA1 endA1 hsdR17* ($r_k^-m_k^+$) *phoA supE44*λ$^-$ *thi-1gyrA96 relA1*	Ref. 67
S. cerevisiae		
W303-1A	*MAT***a** *ade2-1 can1-100 his3-11,15 leu2-3,112 trp1-1 ura3-1*	Ref. 89
GHY57	*pah1Δ::URA3* derivative of W303-1A	Ref. 10
GHY69	*cho1* (CACATG → AAAAAA, −159 to −154) derivative of W303-1A	This study
GHY68	*cho1* (CACATG → AAAAAA, −159 to −154) *pah1Δ::URA3* derivative of W303-1A	This study
GHY70	*cho1Δ::URA3* derivative of W303-1A	This study
RS453	*MAT***a** *ade2-1 his3-11,15 leu2-3,112 trp1-1 ura3-52*	Ref. 90
SS1026	*pah1Δ::TRP1* derivative of RS453	Ref. 13
SS1144	*dgk1Δ::HIS3* derivative of RS453	Ref. 20
SS1147	*dgk1Δ::HIS3 pah1Δ::TRP1* derivative of RS453	Ref. 20

Table 2
Plasmids used in this study

Plasmid	Relevant characteristics	Source/Reference
pRS415	Single-copy *E. coli*/yeast shuttle vector with *LEU2*	Ref. 91
pRS416	Single-copy *E. coli*/yeast shuttle vector with *URA3*	Ref. 91
YEp351	Multicopy *E. coli*/yeast shuttle vector with *LEU2*	Ref. 92
pGH315	pRS415 containing *PAH1* at the XbaI/HindIII sites	Ref. 93
pGH317	YEp351 containing the *pah1Δ::URA3* disruption cassette	Ref. 10
pGH340	pRS416 containing *PAH1* at the XbaI/HindIII sites	This study
pGH440	pRS415 containing *CHO1* with the 1,000-bp promoter at the SacI/HindIII sites	This study
pGH440-900	pGH440 derivative containing the 900-bp *CHO1* promoter	This study
pGH440-800	pGH440 derivative containing the 800-bp *CHO1* promoter	This study
pGH440-700	pGH440 derivative containing the 700-bp *CHO1* promoter	This study
pGH440-600	pGH440 derivative containing the 600-bp *CHO1* promoter	This study
pGH440-500	pGH440 derivative containing the 500-bp *CHO1* promoter	This study
pGH440-400	pGH440 derivative containing the 400-bp *CHO1* promoter	This study
pGH440-300	pGH440 derivative containing the 300-bp *CHO1* promoter	This study
pGH440-200	pGH440 derivative containing the 200-bp *CHO1* promoter	This study
pGH440-100	pGH440 derivative containing the 100-bp *CHO1* promoter	This study
pGH440-0	pGH440 derivative containing the 0-bp *CHO1* promoter	This study
pGH440-190	pGH440 derivative containing the 190-bp *CHO1* promoter	This study
pGH440-170	pGH440 derivative containing the 170-bp *CHO1* promoter	This study
pGH440-150	pGH440 derivative containing the 150-bp *CHO1* promoter	This study
pGH440m	pGH440 with the UAS_{INO} mutation (CACATG → AAAAAA, −159 to −154) in the *CHO1* promoter	This study
pGH442	pGH440 derivative with *cho1Δ::URA3*	This study
YCplac111-*SEC63-GFP*	*SEC63*-GFP fusion inserted into the *CEN/LEU2* vector	Ref. 13

Plasmid constructions

The plasmids used in this work are listed in Table 2. pGH340 was constructed from pRS416 at the XbaI and HindIII sites by insertion of *PAH1* DNA fragments that were released from pGH315 by digestion with XbaI/BglII (2.002 kb) and BglII/HindIII (1.687 kb). pGH440 was constructed from pRS415 at the SacI and HindIII sites by insertion of 2.3-kb *CHO1* DNA (1-kb 5′ UTR + 0.831-kb CDS + 0.5-kb 3′-UTR) that was amplified by PCR from genomic DNA of yeast strain W303-1A (forward primer, GTGGAGCTCTCAGCAGCATCTGGCTGAAA; reverse primer, ATCAAGCTTATTGATGCCATGAAAACCTC). The promoter truncation derivatives of pGH440 were constructed by replacing the SacI-NdeI fragment (2.25 kb) of *CHO1* with those lacking 100–1,000 bp from the 5′-end (forward primers, GTGGAGCTCAAGGAACCAGATGACATGGG, GTGGAGCTCCCGACCCAAATGTAATGGAA, GTGGAGCTCTTTAGAAAACGTCATTTTGA, GTGGAGCTCACAAGCAGTATTAAGCATAA, GTGGAGCTCGATTATAGAGCTTATAGCTA, GTGGAGCTCTGTAAGTATTTGTATATATG, GTGGAGCTCGCATTATAGAAGATATCCCT, GTGGAGCTCACTTTGAACGTTCACACGGC, GTGGAGCTCAAGAGAGATACACCTATTTT, and GTGGAGCTCATGGTTGAATCAGATGAAGA; reverse primer, CTGCCATATGCAAATTCCTCA). pGH440m was produced from pGH440 by replacing the SacI-BsaBI fragment (869 bp) of *CHO1* with that containing the UAS_{INO} mutation (CACATG → AAAAAA, −159 to −154). pGH442, which contains the *cho1Δ::URA3* disruption cassette, was produced from pGH440 by replacing the BstZ17I-NdeI fragment of *CHO1* with the *URA3* gene.

Construction of yeast mutants

The *cho1Δ::URA3* mutant was derived from the yeast strain W303-1A by one-step gene replacement (69). The W303-1A strain was transformed with a 2.9-kb *cho1Δ::URA3* disruption cassette that was released from pGH442 by digestion with SacI and HindIII, and the resulting transformants were selected on the SC-Ura medium supplemented with 1 mM choline. The *cho1Δ* mutant was identified from the Ura$^+$ transformants by choline auxotrophy and by PCR analysis of gene disruption. The *cho1* mutant, which contains a defective *CHO1* UAS_{INO} element, was derived from the *cho1Δ::URA3* mutant by one-step gene replacement. The *cho1Δ* mutant was transformed with a 2.3-kb *CHO1* DNA that was released from pGH440m by digestion with SacI and HindIII, and the resulting transformants were selected on 5-fluoroorotic acid–containing medium. The gene replacement in the 5-fluoroorotic acid–resistant transformant was confirmed by DNA sequencing of the PCR-amplified *CHO1*. The *pah1Δ cho1* mutant was derived from the *cho1Δ* mutant by one-step gene replacement. The

cho1 mutant was transformed with a 3-kb *pah1*Δ*::URA3* disruption cassette that was released from pGH317 by digestion with the XbaI and HindIII. The *pah1*Δ mutation was confirmed from the Ura^+ transformants by temperature sensitivity and PCR analysis of gene disruption.

Preparation of cell extracts

All steps were performed at 4 °C. Yeast cell pellets were resuspended in breaking buffer (50 mM Tris-HCl, pH 7.5, 0.3 M sucrose, 10 mM 2-mercaptoethanol, 0.5 mM phenylmethanesulfonyl fluoride, 1 mM benzamidine, 5 μg/ml aprotinin, 5 μg/ml leupeptin, and 5 μg/ml pepstatin). Glass beads (0.5-mm diameter) were added to the cell suspension, and the mixture was vigorously agitated using the Mini-BeadBeater-16 (Biospec Products). Unbroken cells and glass beads were precipitated by centrifugation at 1,500 × *g* for 10 min, and the supernatant was transferred to a new tube for use as cell extracts. Protein concentration of cell extracts was estimated by the method of Bradford (70) using bovine serum albumin as the standard.

SDS-PAGE and immunoblot analysis

SDS-PAGE (71) and immunoblotting (72–74) using PVDF membrane were performed as described previously. The samples for immunoblotting were normalized to total protein loading. Ponceau S staining was used to monitor the protein transfer from the polyacrylamide gels to the PVDF membrane. Immunoblot analysis of the protein Cho1 was performed with anti-Cho1 antibody raised against the N-terminal portion of the protein (41) at a concentration of 0.25 μg/ml. Goat anti-rabbit IgG antibody conjugated with alkaline phosphatase was used as a secondary antibody at a dilution of 1:5,000. Immune complexes were detected on immunoblots using the enhanced chemifluorescence Western blotting reagents as described by the manufacturer. Images were acquired by fluorimaging analysis. Immunoblotting signals were in the linear range of detectability.

Enzyme assays

All assays were conducted at 30 °C in a total volume of 0.1 ml. PSS activity was measured by following the incorporation of water-soluble [3-^{3}H]serine (10,000 cpm/nmol) into chloroform-soluble [3-^{3}H]PS (75–77). The enzyme reaction contained 50 mM Tris-HCl (pH 8.0), 0.6 mM $MnCl_2$, 4 mM Triton X-100, 0.2 mM CDP–DAG, and 0.5 mM serine (75–77). The enzyme assays were conducted in triplicate, and the average S.D. of the assays was ±5%. The reactions were linear with time and protein concentration. A unit of PSS activity was defined as the amount of enzyme that catalyzed the formation of 1 nmol of product/min.

Radiolabeling and analysis of lipids

The steady-state labeling of lipids with [2-^{14}C]acetate was performed as described previously (43). Lipids were extracted (78) from the radiolabeled cells and then separated by one-dimensional TLC for neutral lipids (79) or phospholipids (80). The resolved lipids were visualized by phosphorimaging and quantified by ImageQuant software using a standard curve of [2-^{14}C]acetate. The identity of radiolabeled lipids was confirmed by comparison with the migration of authentic standards visualized by staining with iodine vapor.

Analysis of PA

PA was analyzed by the fluorometric coupled enzyme assay of Morita *et al.* (81) with minor modifications (82). The cellular lipids were extracted (78), solubilized with purified Triton X-100 (Surfact-Amps), and digested with lipoprotein lipase. The PA derived from glycerol 3-phosphate was coupled to the formation of resorufin with glycerol-3-phosphate oxidase to produce hydrogen peroxide, which is reduced by peroxidase using Amplex Red.

Microscopy

For nuclear/ER membrane morphology analysis, cells were grown at 30 °C and collected at the exponential and stationary phases of growth. The cells were resuspended in a reduced volume of the same medium. For the analysis of lipid droplets, cells were grown in the same medium and collected at the exponential and stationary phases, stained for 30 min with 2 μM BODIPY 493/503, and washed with phosphate-buffered saline (pH 7.4). The average number of cells with normal nuclear/ER membrane structure (*i.e.* round- to oval-shaped circle) or the number of lipid droplets per cell was scored from ≥3 fields of view (≥150 cells). The fluorescence images were observed under a microscope (Nikon Eclipse Ni-U) with a long pass green fluorescent protein filter, captured by the DS-Qi2 camera with the imaging software NIS-Elements BR.

Analyses of data

SigmaPlot software was used for the statistical analysis of data. The p values < 0.05 were taken as a significant difference.

Author contributions—G.-S. H. and G. M. C. designed the study, analyzed the results, and prepared the manuscript. G.-S. H. performed the experiments.

References

1. Carman, G. M., and Han, G.-S. (2011) Regulation of phospholipid synthesis in the yeast *Saccharomyces cerevisiae*. *Annu. Rev. Biochem.* **80,** 859–883
2. Henry, S. A., Kohlwein, S. D., and Carman, G. M. (2012) Metabolism and regulation of glycerolipids in the yeast *Saccharomyces cerevisiae*. *Genetics* **190,** 317–349
3. Habeler, G., Natter, K., Thallinger, G. G., Crawford, M. E., Kohlwein, S. D., and Trajanoski, Z. (2002) YPL.db: the Yeast Protein Localization database. *Nucleic Acids Res.* **30,** 80–83
4. Kumar, A., Agarwal, S., Heyman, J. A., Matson, S., Heidtman, M., Piccirillo, S., Umansky, L., Drawid, A., Jansen, R., Liu, Y., Cheung, K. H., Miller, P., Gerstein, M., Roeder, G. S., and Snyder, M. (2002) Subcellular localization of the yeast proteome. *Genes Dev.* **16,** 707–719
5. Huh, W. K., Falvo, J. V., Gerke, L. C., Carroll, A. S., Howson, R. W., Weissman, J. S., and O'Shea, E. K. (2003) Global analysis of protein localization in budding yeast. *Nature* **425,** 686–691
6. Natter, K., Leitner, P., Faschinger, A., Wolinski, H., McCraith, S., Fields, S., and Kohlwein, S. D. (2005) The spatial organization of lipid synthesis in the yeast *Saccharomyces cerevisiae* derived from large scale green fluorescent protein tagging and high resolution microscopy. *Mol. Cell. Proteomics* **4,** 662–672
7. Karanasios, E., Han, G.-S., Xu, Z., Carman, G. M., and Siniossoglou, S. (2010) A phosphorylation-regulated amphipathic helix controls the mem-

brane translocation and function of the yeast phosphatidate phosphatase. *Proc. Natl. Acad. Sci. U.S.A.* **107,** 17539–17544
8. Karanasios, E., Barbosa, A. D., Sembongi, H., Mari, M., Han, G.-S., Reggiori, F., Carman, G. M., and Siniossoglou, S. (2013) Regulation of lipid droplet and membrane biogenesis by the acidic tail of the phosphatidate phosphatase Pah1p. *Mol. Biol. Cell* **24,** 2124–2133
9. Barbosa, A. D., Sembongi, H., Su, W.-M., Abreu, S., Reggiori, F., Carman, G. M., and Siniossoglou, S. (2015) Lipid partitioning at the nuclear envelope controls membrane biogenesis. *Mol. Biol. Cell* **26,** 3641–3657
10. Han, G.-S., Wu, W.-I., and Carman, G. M. (2006) The *Saccharomyces cerevisiae* lipin homolog is a Mg^{2+}-dependent phosphatidate phosphatase enzyme. *J. Biol. Chem.* **281,** 9210–9218
11. Han, G.-S., Siniossoglou, S., and Carman, G. M. (2007) The cellular functions of the yeast lipin homolog Pah1p are dependent on its phosphatidate phosphatase activity. *J. Biol. Chem.* **282,** 37026–37035
12. Fakas, S., Qiu, Y., Dixon, J. L., Han, G.-S., Ruggles, K. V., Garbarino, J., Sturley, S. L., and Carman, G. M. (2011) Phosphatidate phosphatase activity plays a key role in protection against fatty acid-induced toxicity in yeast. *J. Biol. Chem.* **286,** 29074–29085
13. Santos-Rosa, H., Leung, J., Grimsey, N., Peak-Chew, S., and Siniossoglou, S. (2005) The yeast lipin Smp2 couples phospholipid biosynthesis to nuclear membrane growth. *EMBO J.* **24,** 1931–1941
14. Adeyo, O., Horn, P. J., Lee, S., Binns, D. D., Chandrahas, A., Chapman, K. D., and Goodman, J. M. (2011) The yeast lipin orthologue Pah1p is important for biogenesis of lipid droplets. *J. Cell Biol.* **192,** 1043–1055
15. Irie, K., Takase, M., Araki, H., and Oshima, Y. (1993) A gene, SMP2, involved in plasmid maintenance and respiration in *Saccharomyces cerevisiae* encodes a highly charged protein. *Mol. Gen. Genet.* **236,** 283–288
16. Park, Y., Han, G. S., Mileykovskaya, E., Garrett, T. A., and Carman, G. M. (2015) Altered lipid synthesis by lack of yeast Pah1 phosphatidate phosphatase reduces chronological life span. *J. Biol. Chem.* **290,** 25382–25394
17. Lussier, M., White, A. M., Sheraton, J., di Paolo, T., Treadwell, J., Southard, S. B., Horenstein, C. I., Chen-Weiner, J., Ram, A. F., Kapteyn, J. C., Roemer, T. W., Vo, D. H., Bondoc, D. C., Hall, J., Zhong, W. W., *et al.* (1997) Large scale identification of genes involved in cell surface biosynthesis and architecture in *Saccharomyces cerevisiae*. *Genetics* **147,** 435–450
18. Ruiz, C., Cid, V. J., Lussier, M., Molina, M., and Nombela, C. (1999) A large-scale sonication assay for cell wall mutant analysis in yeast. *Yeast* **15,** 1001–1008
19. Sasser, T., Qiu, Q. S., Karunakaran, S., Padolina, M., Reyes, A., Flood, B., Smith, S., Gonzales, C., and Fratti, R. A. (2012) The yeast lipin 1 orthologue Pah1p regulates vacuole homeostasis and membrane fusion. *J. Biol. Chem.* **287,** 2221–2236
20. Han, G.-S., O'Hara, L., Carman, G. M., and Siniossoglou, S. (2008) An unconventional diacylglycerol kinase that regulates phospholipid synthesis and nuclear membrane growth. *J. Biol. Chem.* **283,** 20433–20442
21. Atkinson, K. D., Jensen, B., Kolat, A. I., Storm, E. M., Henry, S. A., and Fogel, S. (1980) Yeast mutants auxotropic for choline or ethanolamine. *J. Bacteriol.* **141,** 558–564
22. Atkinson, K., Fogel, S., and Henry, S. A. (1980) Yeast mutant defective in phosphatidylserine synthesis. *J. Biol. Chem.* **255,** 6653–6661
23. Nomura, W., Ito, Y., and Inoue, Y. (2017) Role of phosphatidylserine in the activation of Rho1-related Pkc1 signaling in *Saccharomyces cerevisiae*. *Cell. Signal.* **31,** 146–153
24. Dey, P., Su, W. M., Han, G. S., and Carman, G. M. (2017) Phosphorylation of lipid metabolic enzymes by yeast Pkc1 protein kinase C requires phosphatidylserine and diacylglycerol. *J. Lipid Res.* **58,** 742–751
25. Nakamura, H., Miura, K., Fukuda, Y., Shibuya, I., Ohta, A., and Takagi, M. (2000) Phosphatidylserine synthesis required for the maximal tryptophan transport activity in *Saccharomyces cerevisiae*. *Biosci. Biotechnol. Biochem.* **64,** 167–172
26. Hamamatsu, S., Shibuya, I., Takagi, M., and Ohta, A. (1994) Loss of phosphatidylserine synthesis results in aberrant solute sequestration and vacuolar morphology in *Saccharomyces cerevisiae*. *FEBS Lett.* **348,** 33–36
27. Sun, Y., and Drubin, D. G. (2012) The functions of anionic phospholipids during clathrin-mediated endocytosis site initiation and vesicle formation. *J. Cell Sci.* **125,** 6157–6165
28. Klig, L. S., Homann, M. J., Carman, G. M., and Henry, S. A. (1985) Coordinate regulation of phospholipid biosynthesis in *Saccharomyces cerevisiae*: pleiotropically constitutive *opi1* mutant. *J. Bacteriol.* **162,** 1135–1141
29. Poole, M. A., Homann, M. J., Bae-Lee, M. S., and Carman, G. M. (1986) Regulation of phosphatidylserine synthase from *Saccharomyces cerevisiae* by phospholipid precursors. *J. Bacteriol.* **168,** 668–672
30. Bailis, A. M., Poole, M. A., Carman, G. M., and Henry, S. A. (1987) The membrane-associated enzyme phosphatidylserine synthase of yeast is regulated at the level of mRNA abundance. *Mol. Cell. Biol.* **7,** 167–176
31. Bailis, A. M., Lopes, J. M., Kohlwein, S. D., and Henry, S. A. (1992) Cis and trans regulatory elements required for regulation of the *CHO1* gene of *Saccharomyces cerevisiae*. *Nucleic Acids Res.* **20,** 1411–1418
32. Homann, M. J., Bailis, A. M., Henry, S. A., and Carman, G. M. (1987) Coordinate regulation of phospholipid biosynthesis by serine in *Saccharomyces cerevisiae*. *J. Bacteriol.* **169,** 3276–3280
33. Iwanyshyn, W. M., Han, G.-S., and Carman, G. M. (2004) Regulation of phospholipid synthesis in *Saccharomyces cerevisiae* by zinc. *J. Biol. Chem.* **279,** 21976–21983
34. Homann, M. J., Poole, M. A., Gaynor, P. M., Ho, C.-T., and Carman, G. M. (1987) Effect of growth phase on phospholipid biosynthesis in *Saccharomyces cerevisiae*. *J. Bacteriol.* **169,** 533–539
35. Lamping, E., Lückl, J., Paltauf, F., Henry, S. A., and Kohlwein, S. D. (1994) Isolation and characterization of a mutant of *Saccharomyces cerevisiae* with pleiotropic deficiencies in transcriptional activation and repression. *Genetics* **137,** 55–65
36. Carman, G. M., and Henry, S. A. (2007) Phosphatidic acid plays a central role in the transcriptional regulation of glycerophospholipid synthesis in *Saccharomyces cerevisiae*. *J. Biol. Chem.* **282,** 37293–37297
37. Pascual, F., Soto-Cardalda, A., and Carman, G. M. (2013) *PAH1*-encoded phosphatidate phosphatase plays a role in the growth phase- and inositol-mediated regulation of lipid synthesis in *Saccharomyces cerevisiae*. *J. Biol. Chem.* **288,** 35781–35792
38. Soto-Cardalda, A., Fakas, S., Pascual, F., Choi, H. S., and Carman, G. M. (2012) Phosphatidate phosphatase plays role in zinc-mediated regulation of phospholipid synthesis in yeast. *J. Biol. Chem.* **287,** 968–977
39. Pascual, F., and Carman, G. M. (2013) Phosphatidate phosphatase, a key regulator of lipid homeostasis. *Biochim. Biophys. Acta* **1831,** 514–522
40. Lee, K. S., Irie, K., Gotoh, Y., Watanabe, Y., Araki, H., Nishida, E., Matsumoto, K., and Levin, D. E. (1993) A yeast mitogen-activated protein kinase homolog (Mpk1p) mediates signalling by protein kinase C. *Mol. Cell. Biol.* **13,** 3067–3075
41. Choi, H.-S., Han, G.-S., and Carman, G. M. (2010) Phosphorylation of yeast phosphatidylserine synthase by protein kinase A: identification of Ser^{46} and Ser^{47} as major sites of phosphorylation. *J. Biol. Chem.* **285,** 11526–11536
42. Choi, H.-S., Sreenivas, A., Han, G.-S., and Carman, G. M. (2004) Regulation of phospholipid synthesis in the yeast *cki1*Δ *eki1*Δ mutant defective in the Kennedy pathway. The *CHO1*-encoded phosphatidylserine synthase is regulated by mRNA stability. *J. Biol. Chem.* **279,** 12081–12087
43. Morlock, K. R., Lin, Y.-P., and Carman, G. M. (1988) Regulation of phosphatidate phosphatase activity by inositol in *Saccharomyces cerevisiae*. *J. Bacteriol.* **170,** 3561–3566
44. Kelley, M. J., Bailis, A. M., Henry, S. A., and Carman, G. M. (1988) Regulation of phospholipid biosynthesis in *Saccharomyces cerevisiae* by inositol: inositol is an inhibitor of phosphatidylserine synthase activity. *J. Biol. Chem.* **263,** 18078–18085
45. Loewen, C. J. R., Gaspar, M. L., Jesch, S. A., Delon, C., Ktistakis, N. T., Henry, S. A., and Levine, T. P. (2004) Phospholipid metabolism regulated by a transcription factor sensing phosphatidic acid. *Science* **304,** 1644–1647
46. Greenberg, M. L., and Lopes, J. M. (1996) Genetic regulation of phospholipid biosynthesis in *Saccharomyces cerevisiae*. *Microbiol. Rev.* **60,** 1–20
47. Carman, G. M., and Henry, S. A. (1999) Phospholipid biosynthesis in the yeast *Saccharomyces cerevisiae* and interrelationship with other metabolic processes. *Prog. Lipid Res.* **38,** 361–399

48. O'Hara, L., Han, G.-S., Peak-Chew, S., Grimsey, N., Carman, G. M., and Siniossoglou, S. (2006) Control of phospholipid synthesis by phosphorylation of the yeast lipin Pah1p/Smp2p Mg^{2+}-dependent phosphatidate phosphatase. *J. Biol. Chem.* **281,** 34537–34548
49. Hosaka, K., Murakami, T., Kodaki, T., Nikawa, J., and Yamashita, S. (1990) Repression of choline kinase by inositol and choline in *Saccharomyces cerevisiae*. *J. Bacteriol.* **172,** 2005–2012
50. Morash, S. C., McMaster, C. R., Hjelmstad, R. H., and Bell, R. M. (1994) Studies employing *Saccharomyces cerevisiae cpt1* and *ept1* null mutants implicate the *CPT1* gene in coordinate regulation of phospholipid biosynthesis. *J. Biol. Chem.* **269,** 28769–28776
51. Kersting, M. C., Choi, H. S., and Carman, G. M. (2004) Regulation of the yeast *EKI1*-encoded ethanolamine kinase by inositol and choline. *J. Biol. Chem.* **279,** 35353–35359
52. McMaster, C. R., and Bell, R. M. (1994) Phosphatidylcholine biosynthesis via the CDP-choline pathway in *Saccharomyces cerevisiae*: multiple mechanisms of regulation. *J. Biol. Chem.* **269,** 14776–14783
53. Anderson, M. S., and Lopes, J. M. (1996) Carbon source regulation of *PIS1* gene expression in *Saccharomyces cerevisiae* involves the *MCM1* gene and the two-component regulatory gene, *SLN1*. *J. Biol. Chem.* **271,** 26596–26601
54. Donahue, T. F., and Henry, S. A. (1981) Myo-inositol-1-phosphate synthase: characteristics of the enzyme and identification of its structural gene in yeast. *J. Biol. Chem.* **256,** 7077–7085
55. Hirsch, J. P., and Henry, S. A. (1986) Expression of the *Saccharomyces cerevisiae* inositol-1-phosphate synthase (*INO1*) gene is regulated by factors that affect phospholipid synthesis. *Mol. Cell. Biol.* **6,** 3320–3328
56. Hasslacher, M., Ivessa, A. S., Paltauf, F., and Kohlwein, S. D. (1993) Acetyl-CoA carboxylase from yeast is an essential enzyme and is regulated by factors that control phospholipid metabolism. *J. Biol. Chem.* **268,** 10946–10952
57. Schüller, H. J., Hahn, A., Tröster, F., Schütz, A., and Schweizer, E. (1992) Coordinate genetic control of yeast fatty acid synthase genes *FAS1* and *FAS2* by an upstream activation site common to genes involved in membrane lipid biosynthesis. *EMBO J.* **11,** 107–114
58. Han, G.-S., O'Hara, L., Siniossoglou, S., and Carman, G. M. (2008) Characterization of the yeast *DGK1*-encoded CTP-dependent diacylglycerol kinase. *J. Biol. Chem.* **283,** 20443–20453
59. Fei, W., Shui, G., Zhang, Y., Krahmer, N., Ferguson, C., Kapterian, T. S., Lin, R. C., Dawes, I. W., Brown, A. J., Li, P., Huang, X., Parton, R. G., Wenk, M. R., Walther, T. C., and Yang, H. (2011) A role for phosphatidic acid in the formation of "supersized" lipid droplets. *PLoS Genet.* **7,** e1002201
60. Miner, G. E., Starr, M. L., Hurst, L. R., and Fratti, R. A. (2017) Deleting the DAG kinase Dgk1 augments yeast vacuole fusion through increased Ypt7 activity and altered membrane fluidity. *Traffic* **18,** 315–329
61. Wu, W.-I., and Carman, G. M. (1996) Regulation of phosphatidate phosphatase activity from the yeast *Saccharomyces cerevisiae* by phospholipids. *Biochemistry* **35,** 3790–3796
62. Bae-Lee, M., and Carman, G. M. (1990) Regulation of yeast phosphatidylserine synthase and phosphatidylinositol synthase activities by phospholipids in Triton X-100/phospholipid mixed micelles. *J. Biol. Chem.* **265,** 7221–7226
63. Su, W.-M., Han, G.-S., Casciano, J., and Carman, G. M. (2012) Protein kinase A-mediated phosphorylation of Pah1p phosphatidate phosphatase functions in conjunction with the Pho85p-Pho80p and Cdc28p-cyclin B kinases to regulate lipid synthesis in yeast. *J. Biol. Chem.* **287,** 33364–33376
64. Kinney, A. J., and Carman, G. M. (1988) Phosphorylation of yeast phosphatidylserine synthase *in vivo* and *in vitro* by cyclic AMP-dependent protein kinase. *Proc. Natl. Acad. Sci. U.S.A.* **85,** 7962–7966
65. Chang, Y.-F., and Carman, G. M. (2008) CTP synthetase and its role in phospholipid synthesis in the yeast *Saccharomyces cerevisiae*. *Prog. Lipid Res.* **47,** 333–339
66. Rose, M. D., Winston, F., and Heiter, P. (1990) *Methods in Yeast Genetics: A Laboratory Course Manual*, Cold Spring Harbor Laboratory Press, Cold Spring Harbor, NY
67. Sambrook, J., Fritsch, E. F., and Maniatis, T. (1989) *Molecular Cloning: A Laboratory Manual*, 2nd Ed., Cold Spring Harbor Laboratory, Cold Spring Harbor, NY
68. Innis, M. A., and Gelfand, D. H. (1990) in *PCR Protocols: A Guide to Methods and Applications* (Innis, M. A., Gelfand, D. H., Sninsky, J. J., and White, T. J., eds) pp. 3–12, Academic Press, Inc., San Diego
69. Rothstein, R. (1991) Targeting, disruption, replacement, and allele rescue: integrative DNA transformation in yeast. *Methods Enzymol.* **194,** 281–301
70. Bradford, M. M. (1976) A rapid and sensitive method for the quantitation of microgram quantities of protein utilizing the principle of protein-dye binding. *Anal. Biochem.* **72,** 248–254
71. Laemmli, U. K. (1970) Cleavage of structural proteins during the assembly of the head of bacteriophage T4. *Nature* **227,** 680–685
72. Guengerich, F. P., Wang, P., and Davidson, N. K. (1982) Estimation of isozymes of microsomal cytochrome P-450 in rats, rabbits, and humans using immunochemical staining coupled with sodium dodecyl sulfate-polyacrylamide gel electrophoresis. *Biochemistry* **21,** 1698–1706
73. Burnette, W. (1981) Western blotting: electrophoretic transfer of proteins from sodium dodecyl sulfate-polyacrylamide gels to unmodified nitrocellulose and radiographic detection with antibody and radioiodinated protein A. *Anal. Biochem.* **112,** 195–203
74. Haid, A., and Suissa, M. (1983) Immunochemical identification of membrane proteins after sodium dodecyl sulfate-polyacrylamide gel electrophoresis. *Methods Enzymol.* **96,** 192–205
75. Carman, G. M., and Matas, J. (1981) Solubilization of microsomal-associated phosphatidylserine synthase and phosphatidylinositol synthase from *Saccharomyces cerevisiae*. *Can. J. Microbiol.* **27,** 1140–1149
76. Bae-Lee, M. S., and Carman, G. M. (1984) Phosphatidylserine synthesis in *Saccharomyces cerevisiae*: purification and characterization of membrane-associated phosphatidylserine synthase. *J. Biol. Chem.* **259,** 10857–10862
77. Carman, G. M., and Bae-Lee, M. (1992) Phosphatidylserine synthase from yeast. *Methods Enzymol.* **209,** 298–305
78. Bligh, E. G., and Dyer, W. J. (1959) A rapid method of total lipid extraction and purification. *Can. J. Biochem. Physiol.* **37,** 911–917
79. Henderson, R. J., and Tocher, D. R. (1992) in *Lipid Analysis* (Hamilton, R. J., and Hamilton, S., eds) pp. 65–111, IRL Press, New York
80. Vaden, D. L., Gohil, V. M., Gu, Z., and Greenberg, M. L. (2005) Separation of yeast phospholipids using one-dimensional thin-layer chromatography. *Anal. Biochem.* **338,** 162–164
81. Morita, S. Y., Ueda, K., and Kitagawa, S. (2009) Enzymatic measurement of phosphatidic acid in cultured cells. *J. Lipid Res.* **50,** 1945–1952
82. Hassaninasab, A., Han, G.-S., and Carman, G. M. (2017) Tips on the analysis of phosphatidic acid by the fluorometric coupled enzyme assay. *Anal. Biochem.* **526,** 69–70
83. Chae, M., Han, G.-S., and Carman, G. M. (2012) The *Saccharomyces cerevisiae* actin patch protein App1p is a phosphatidate phosphatase enzyme. *J. Biol. Chem.* **287,** 40186–40196
84. Chae, M., and Carman, G. M. (2013) Characterization of the yeast actin patch protein App1p phosphatidate phosphatase. *J. Biol. Chem.* **288,** 6427–6437
85. Toke, D. A., Bennett, W. L., Dillon, D. A., Wu, W.-I., Chen, X., Ostrander, D. B., Oshiro, J., Cremesti, A., Voelker, D. R., Fischl, A. S., and Carman, G. M. (1998) Isolation and characterization of the *Saccharomyces cerevisiae DPP1* gene encoding for diacylglycerol pyrophosphate phosphatase. *J. Biol. Chem.* **273,** 3278–3284
86. Toke, D. A., Bennett, W. L., Oshiro, J., Wu, W.-I., Voelker, D. R., and Carman, G. M. (1998) Isolation and characterization of the *Saccharomyces cerevisiae LPP1* gene encoding a Mg^{2+}-independent phosphatidate phosphatase. *J. Biol. Chem.* **273,** 14331–14338
87. Larson, T. J., and Dowhan, W. (1976) Ribosomal-associated phosphatidylserine synthetase from *Escherichia coli*: purification by substrate-specific elution from phosphocellulose using cytidine 5′-diphospho-1,2-diacyl-*sn*-glycerol. *Biochemistry* **15,** 5212–5218
88. Vance, J. E. (1998) Eukaryotic lipid-biosynthetic enzymes: the same but not the same. *Trends Biochem. Sci.* **23,** 423–428

89. Ostrander, D. B., O'Brien, D. J., Gorman, J. A., and Carman, G. M. (1998) Effect of CTP synthetase regulation by CTP on phospholipid synthesis in *Saccharomyces cerevisiae*. *J. Biol. Chem.* **273,** 18992–19001
90. Wimmer, C., Doye, V., Grandi, P., Nehrbass, U., and Hurt, E. C. (1992) A new subclass of nucleoporins that functionally interact with nuclear pore protein NSP1. *EMBO J.* **11,** 5051–5061
91. Sikorski, R. S., and Hieter, P. (1989) A system of shuttle vectors and yeast host strains designed for efficient manipulation of DNA in *Saccharomyces cerevisiae*. *Genetics* **122,** 19–27
92. Hill, J. E., Myers, A. M., Koerner, T. J., and Tzagoloff, A. (1986) Yeast/*E. coli* shuttle vectors with multiple unique restriction sites. *Yeast* **2,** 163–167
93. Choi, H.-S., Su, W.-M., Morgan, J. M., Han, G.-S., Xu, Z., Karanasios, E., Siniossoglou, S., and Carman, G. M. (2011) Phosphorylation of phosphatidate phosphatase regulates its membrane association and physiological functions in *Saccharomyces cerevisiae:* identification of Ser^{602}, Thr^{723}, and Ser^{744} as the sites phosphorylated by *CDC28* (*CDK1*)-encoded cyclin-dependent kinase. *J. Biol. Chem.* **286,** 1486–1498

Yeast *PAH1*-encoded phosphatidate phosphatase controls the expression of *CHO1*-encoded phosphatidylserine synthase for membrane phospholipid synthesis

Gil-Soo Han and George M. Carman

J. Biol. Chem. 2017, 292:13230-13242.
doi: 10.1074/jbc.M117.801720 originally published online July 3, 2017